ELSEVIER

Journal of Nuclear Materials 283–287 (2000) 992–996

journal of nuclear materials

www.elsevier.nl/locate/jnucmat

Confocal microscopy–fracture reconstruction and finite element modeling characterization of local cleavage toughness in a ferritic/martensitic steel in subsized Charpy V-notch impact tests

T. Yamamoto [a,b,*], G.R. Odette [b], G.E. Lucas [b], H. Matsui [a]

[a] *Institute for Materials Research, Tohoku University, 2-1-1 Katahira, Aoba-ku, 980-8577 Sendai, Japan*
[b] *Department of Mechanical and Environmental Engineering, University of California, Santa Barbara, CA 93106-5070, USA*

Abstract

The confocal microscopy (CM)–fracture reconstruction (FR) method, coupled with scanning electron microscopy (SEM) fractography, was used to measure the critical notch deformation conditions at cleavage initiation for two subsized Charpy V-notch (CVN) specimen geometries of Japan ferritic/martensitic steel (JFMS). A new method was developed to permit FR of notched specimens. Three-dimensional finite element analysis (FEA) simulations of the notch and specimen deformation were used to estimate values of critical micro-cleavage fracture stress, σ^*, and critical stressed area, A^*. Since σ^*–A^* is independent of size and geometry, it provides a fundamental local measure of cleavage toughness.

1. Introduction

Due to very limited irradiation volumes in present and future irradiation facilities, specimen miniaturization is required for testing candidate structural materials for fusion reactors. The fracture energy–temperature curves derived from Charpy V-notch (CVN)-type tests depend explicitly on specimen size and geometry [1–4]. Thus, extracting more fundamentally and structurally useful mechanical properties from such tests requires good physical understanding of the combined macromechanics and micromechanics of fracture. Fundamental properties should be independent of explicit test factors, such as specimen size and geometry. Previous studies have shown that local conditions leading to cleavage fracture can be characterized by a critical tensile stress, σ^*, operating over a critical area, A^* (or volume V^*), ahead of the crack or notch tip. The σ^*–A^* is mediated by both microstructural features (i.e., large boundary carbides) that act as trigger sites for cleavage microcrack formation and the intrinsic toughness of the metal matrix controlling the subsequent propagation of the microcracks. More complex processes associated with the formation and ultimate instability of a population of microcracks in the local process zone also play a role in determining σ^*–A^* [5].

Experimental estimates of σ^*–A^* can be determined from tests on small specimens from either the impact load–displacement curves or the notch deformation at the cleavage initiation using finite element analysis (FEA) simulations of the crack tip fields. The load–displacement curves are generally inferred from the corresponding load–time record. However, large inertial oscillations, particularly in small specimens tested at high impact velocity, often obscure the pertinent load–time trace. More generally, however, critical notch deformation can also be determined using the confocal microscopy (CM)–fracture reconstruction (FR) method. The CM–FR method has proven highly successful for

* Corresponding author. Tel.: +81-22 215 2067; fax: +81-22 215 2066.
E-mail address: yamataku@fusion.imr.tohoku.ac.jp (T. Yamamoto).

0022-3115/00/$ - see front matter
PII: S0022-3115(00)00385-8

fatigue pre-crack-type specimens [6–10]. In this case, FR is facilitated by the existence of one or more pairs of flat reference surfaces. In principle, the CM–FR technique can also be applied to notched impact specimens. However, this application requires development of new FR methods that do not rely on flat fatigue pre-crack reference surfaces. The objective of this research was to develop these FR methods and to apply them to various sized CVN-type specimens.

2. Experiment

The topographic maps of conjugate fracture surfaces are obtained using CM coupled with SEM fractography. Each point in a fracture surface retains the deformation accumulated up to the point of separation from its conjugate point on the other fracture surface. Hence, when the broken specimen halves are reconfigured to their original, pre-test position, the locally deformed conjugate fracture surfaces overlap. FR is carried out by subsequent numerical separation of the broken half-specimens that faithfully follows the macroscopic displacement trajectory of the actual test. The locations and sequence of local material separations are revealed by the corresponding locations and sequence of separation of the previously overlapped surfaces. Conjugate locations with smaller deformation, and hence with less overlap, separate before more highly deformed regions. The sequence of local separations ends at a point of specimen displacement corresponding to macroscopic fracture.

In a bend test, the local displacement of a point depends on the rotation about and the distance from the center of rotation, as well as the macroscopic load point displacement. Edsinger and Odette developed a so-called 'warping' technique to relate the load point to local displacements in pre-cracked specimens based on a detailed FEA [6,7]. The technique, including the suite of numerical algorithms for both CM and FR, is described elsewhere [7]. In this case, the undeformed pre-cracked reference surfaces displace and rotate around a fixed point ahead of crack tip, and the displacement and rotation is proportional to crack-tip blunting. In this work, the FR method was extended to develop a corresponding reference surface approach for notched specimens, based on three-dimensional FEA.

Two subsized CVN-type specimen configurations of Japan ferritic/martensitic steel (JFMS) were tested: (a) a $3.3 \times 3.3 \times 23.8$ mm^3 bar with a notch depth of 0.51 mm termed as 3.3CVN; and (b) a $1 \times 1 \times 20$ mm^3 bar with a notch depth of 0.3 mm, termed as 1CVN. The opening angle of the notch was 30° in both cases. The root radius of the notch was 0.032 ± 0.003 mm in the 3.3CVN and 0.024 ± 0.002 mm in the 1CVN. The ductile-to-brittle transition temperatures, indexed at the mean of the lower and upper shelf energies, were −33°C for the 3.3CVN and −48°C for the 1CVN. Further details of the material, specimens and tests as well as the impact properties are described elsewhere [2].

An FEA of the CVN specimens was carried out with the ABAQUS code using a three-dimensional quarter-symmetry mesh. The analysis used a constitutive equation $\sigma(T, \varepsilon, \dot{\varepsilon})$ that was derived from uniaxial tensile tests

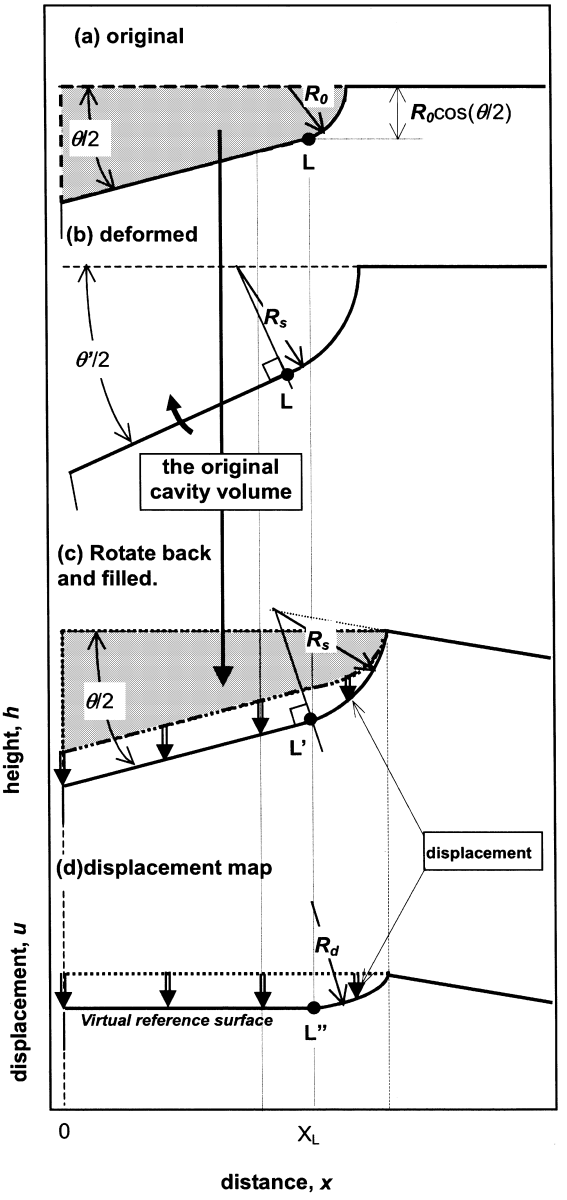

Fig. 1. Procedure to extract the displacement–distance curve from the height–distance of the deformed notch surface.

at strain rates ranging from 1×10^{-4} to 4×10^{-2} s^{-1} at temperatures from −120°C to −20°C that was within 4% error of the experimental flow stress. The simulated load–displacement curves for both specimens were consistent with measured values, supporting the application of the constitutive equation at high strain rates. The FEA provided both macroscopic displacements, rotations and deformation as well as the area (A) within specified normal stress (σ_{yy}) contours at the notch tip, $A(\sigma_{yy})$.

3. Results and discussion

A reference surface is needed to determine appropriate displacements and rotations in an FR. FEA showed that a virtual reference surface that is equivalent to a pre-crack surface can be constructed from a V-notch, as illustrated in Fig. 1. First, the notch profile in the deformed specimen in Fig. 1(b) is rotated until the undeformed part of the profile, to the left of the tangent point, marked L, is parallel to the corresponding pre-test

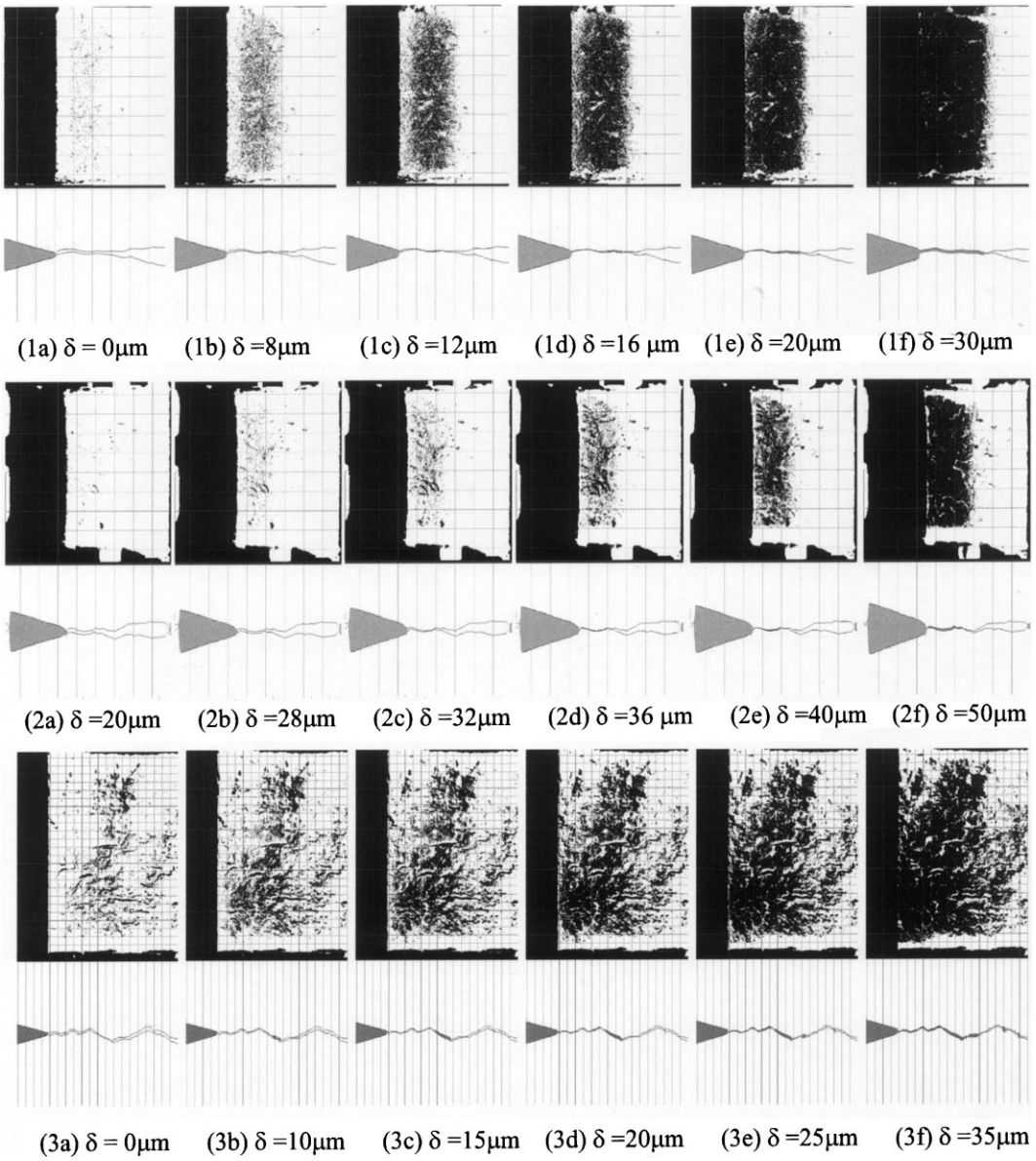

Fig. 2. FR results of JFMS CVN specimens as a function of notch opening displacement, δ. (1a–f) 1CVN tested at −100°C, (2a–f)1CVN tested at −60°C and (3a–f) 3.3CVN tested at −60°C. Each series of figures shows a view of fracture evolution on the crack plane (upper) and fracture surface profiles (lower). Separation is shown as black/shaded areas, respectively.

notch profile shown in Fig. 1(a). the notch profiles are then displaced so that their tips coincide, as shown in Fig. 1(c). The distances between the rotated-displaced pre- and post- test profiles are used to construct a virtual reference surface profile by imposing the same displacements from the notch centerline, as shown in Fig. 1(d). Note that the virtual profile at the tip is not a realistic representation of the highly deformed region very close to the notch tip. However, the undeformed part of the virtual reference surface can be used in the standard pre-crack 'warping' procedure.

Fig. 2 shows representative FR results. The top views, looking down on the fracture plane, show the evolution of the separated regions (in black) with notch opening, δ. The notch profiles, averaged over the fracture region, show the corresponding deformation of the notch and the evolution of the overlap-separation in front of the notch. In the case of the 1CVN specimen tested at -100°C (near the lower shelf of the impact energy–temperature curve) in Figs. 2(1a–f), cleavage microcracking begins at a δ of a few microns over the peak stress region from about 60 to 200 μm, and a macroscopic cleavage pop-in crack is arrested at $\delta \cong 16$ μm. The peak in the derivative of the number of separated pixels in the fracture region was used to define the cleavage initiation at a critical $\delta^* \cong 14$ μm. The FR images closely correspond to SEM fractographs, including the presence of ductile shear lips at the sides of the specimen and a star-shaped initiation site in the center about 200 μm ahead of the notch tip.

Figs. 2(2a–f) show FR results for 1CVN tested at -60°C, which absorbed 25% of the upper shelf energy. In this case, the initial cleavage microcracking is observed between $\delta \cong 32$–36 μm. Based on the peak in the derivative criteria, cleavage initiation occurs at $\delta^* \cong 40$ μm. Figs. 2(3a–f) show the FR results for a 3.3CVN tested at -60°C which absorbed about 7% of the upper shelf energy. The black areas on the fracture surface at $\delta = 0$ μm are 'noise' and represent the limitations of the method, which are primarily associated with post-pop-in specimen distortions and cumulative errors in the CM and FR process, like conjugate surface alignment. Cleavage initiated at $\delta \cong 10$ μm, and a pop-in was complete at $\delta \cong 18$ μm. Additional displacement resulted in additional crack extension through almost the entire specimen, leaving only side and back shear lips.

These trends are consistent with expectations. The 1CVN test at -100°C was the most brittle in terms of absorbed energy and δ^*. The smaller 1CVN specimen was about two times more ductile than the 3.3CVN tested at -60°C in terms of δ^*. At the same test temperature, the 3.3CVN absorbed a smaller fraction of the upper shelf energy than the 1CVN. It should be noted that the absorbed energy includes ductile tearing of the post pop-in ligament. Thus, the smaller fractional area of the cleavage pop-in in the 1CVN specimen partially contributes to a larger proportion of post-initiation plastic work in the total absorbed impact energy compared to the 3.3CVN specimen. While this explicit test- and geometry-dependent effect is not germane to the basic fracture process, it must be included in any model of the overall absorbed energy–temperature curve.

The δ at cleavage initiation is related to a corresponding load point displacement Δ. Fig. 3 shows the distribution of the stress component normal to the crack plane (σ_{yy}) in the range of the critical Δ (mm) to initiate cleavage. The profiles are roughly similar, but the smaller 1CVN tests have a slightly higher stress extending further from the notch tip. Fig. 4 plots the corresponding average area, A, as a function of the σ_{yy} defining the stress contour. The average A is defined as

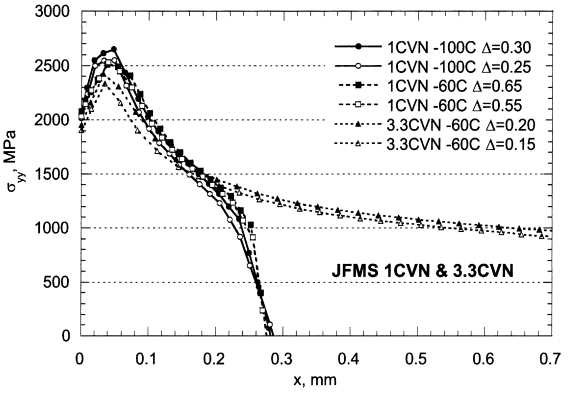

Fig. 3. The tensile stress fields ahead of the V-notch in both 1 and 3.3 mm CVN specimens.

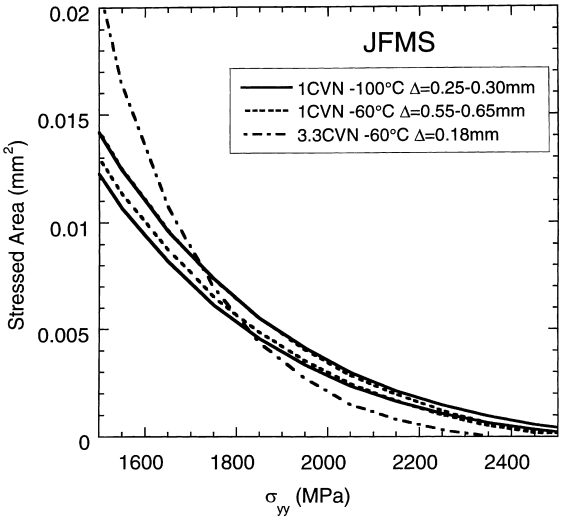

Fig. 4. Stressed area as a function of the value of σ_{yy} defining the stress contour.

the total stressed volume within σ_{yy} divided by specimen thickness. To minimize the effect of expected scatter, the curve for mean δ^* in the 3CVN test at -60°C is shown. The lines cross $\sigma^* \approx 1850 \pm 100$ MPa and $A^* \approx 5 \pm 1.5 \times 10^{-9}$ m^2. These values are in reasonable agreement with previous estimates of local fracture properties for these types of steels. However, additional redundant testing using a range of specimen geometry, including sharp pre-cracks, will be needed to verify these results.

4. Conclusion

A virtual reference surface CM–FR method has been developed for V-notched specimens based on finite element analyses. The new method was applied to characterize the critical notch deformation δ^* and critical corresponding load line displacement Δ^* at cleavage initiation in 1 and 3.3 mm notched CVN-type impact specimens tested at -60°C and -100°C. The CM–FR also provided insight into the microscopic sequence of events preceding cleavage and the stress distributions ahead of the deformed notch at cleavage initiation. Analysis of the stress distributions showed that local fracture parameters of critical stress $\sigma^* = 1800 \pm 100$ MPa and critical area $A^* = 5 \pm 1.5 \times 10^{-9}$ m^3 provide a size- and temperature-independent criterion for cleavage initiation.

Acknowledgements

The authors are grateful to Professor Kurishita, Tohoku University, for providing the fractured test pieces. The authors are grateful for the researcher-exchange program supported by the Ministry of Education, Science, Sports and Culture of Japan. The work was supported in part by the US Department of Energy Grant # DE-FG03-87ER-52143.

References

[1] G.E. Lucas, G.R. Odette, J.W. Sheckherd, P. McConnell, J. Perrin, in: ASTM STP, vol. 888, American Society for Testing and Materials, 1986, p. 304.
[2] H. Kurishita, H. Kayano, M. Narui, M. Yamazaki, Y. Kano, I. Shibahara, Mater. Trans. JIM 34 (1993) 1042.
[3] M.A. Sokolov, R.K. Nanstad, in: ASTM STP, vol. 1270, American Society for Testing and Materials, 1996, p. 384.
[4] G.E. Lucas, G.R. Odette, K. Edsinger, B.D. Wirth, J.W. Sheckherd, in: ASTM STP, vol. 1270, American Society for Testing and Materials, 1996, p. 790.
[5] G.R. Odette, J. Nucl. Mater. 215 (1994) 45.
[6] G.R. Odette, K. Edisinger, G.E. Lucas, E. Donahue, in: ASTM STP, vol. 1329, American Society for Testing and Materials, 1998.
[7] K. Edsinger, Fracture Reconstruction and Advanced Micromechanical Modeling of Structural Steels, PhD thesis, University of California, Santa Barbara, 1995.
[8] K. Edsinger, G.R. Odette, G.E. Lucas, in: Proceedings of the IEA International Symposium on Miniaturized Specimens for Testing of Irradiated Materials, Julich, Germany, September 1994.
[9] K. Edsinger, G.R. Odette, G.E. Lucas, B.D. Wirth, in: ASTM STP, vol. 1270, American Society for Testing and Materials, 1996, p. 670.
[10] B.D. Wirth, K. Edsinger, G.R. Odette, G.E. Lucas, in: ASTM STP, vol. 1270, American Society for Testing and Materials, 1996, p. 706.